

# INTERIM REPORT

## Wind-Induced Loads On Roof Overhangs

Florida Department of Business and Professional Regulation

Florida Building Commission

And

Laboratory for Wind Engineering Research (LWER), Extreme Events Institute  
(EEI)

Florida International University (FIU)

**Project PI:** Ioannis Zisis, Associate Professor, CEE, Florida International University, USA

**Project Co-PI:** Ted Stathopoulos, Professor, BCEE, Concordia University, Canada

**Graduate Student:** Karim Mostafa, CEE, Florida International University, USA

**Date:** February 2021

## Contents

1. Introduction .....	1
2. Previous studies on the effect of wind loads on roof overhangs .....	1
2.1. Wind induced forces on eaves of low buildings with higher slope roof .....	2
2.2. The assessment of wind loads on roof overhang with different lengths .....	2
2.3. Field monitoring under extreme events and wind tunnel study of wind effects on roof overhangs .....	3
2.4. Numerical simulations to study the wind loads on overhangs .....	4
2.5. Effect of overhangs on wind pressures on low-rise hip roof buildings.....	4
2.6. Experimental study of wind loads on gable roofs of low-rise buildings with overhangs	4
2.7. Wind load on overhangs in a low gable building in presence of free-standing wall .....	5
3. Limitations of previous studies and recommendations .....	6
4. Proposed experimental setup .....	7
4.1. Model layouts and dimensions .....	7
4.2. Instrumentation and test protocol.....	9
References.....	12

## List of Figures

Figure 1 Sketch shows the side view and elevation for the building model.....	3
Figure 2 Configuration A model layout (a) Plan View (b) Side View (c) Elevation View.....	8
Figure 3 Configuration B model layout (a) Plan View (b) Side View (c) Elevation View (all dimensions are at model-scale).....	8
Figure 4 Pressure taps instrumentation on configuration A model (a) Roof (b) Longitudinal and Side Walls (c) Longitudinal overhang (d) Side overhang. ....	10
Figure 5 Pressure taps instrumentation on configuration B model (a) Roof (b) Longitudinal and Side Walls (c) Longitudinal overhang (d) Side overhang. ....	11

## List of Tables

Table 1 Summary of parameters and findings in previous studies .....	5
Table 2 Testing parameters scale factors .....	9
Table 3 Prototype and scaled model dimensions .....	9

## **1. Introduction**

An overhang is an unenclosed continuation of the roof surface. Particularly on low-rise residential applications, overhangs may be open or covered by a soffit and may be cantilevered or supported. Most of the foundational belief about overhangs seems to suggest that overhangs extend no more than 2ft, whereas, in Florida, overhangs are often much longer and are necessary for energy efficiency and livability in this semi-tropical climate. Overhangs in Florida can be cantilevered 6ft or more, or supported, as on a terrace or porch, for 10 to 12ft or more.

Low-rise buildings are greatly affected by extreme wind events. The risk of wind-induced failure is particularly increased on roofs and roof overhangs. Low-rise buildings are greatly affected by extreme wind events. The risk of wind-induced failure is particularly increased on roofs and roof overhangs. The latter are commonly used in residential and industrial buildings for weather protection against wind, snow, rain and sun. Extended overhangs resemble a roof extension similar to a canopy or a patio cover that is attached to the main structure. Recent studies showed that canopies may experience lower wind loads compared to those specified for roof overhangs on ASCE 7 (Zisis and Stathopoulos 2010, Candelario et al. 2014, Zisis et al. 2017).

ASCE 7-16 (2017) provides methods for analysis of the loads on overhangs, both for main wind force resisting systems (MWFRS) and component and cladding (C&C) loads, but the commentary does not provide any information as to the maximum length of overhang for which this analysis is valid. In section 30.9, it states that the pressure on the bottom covering of the roof overhang is the external pressure coefficient on the adjacent wall surface. This particular assumption was adopted more recently in the ASCE 7-16 (2017). In earlier versions of the ASCE 7 (2010), the overhang pressures considered the net pressure applied on these elements from simultaneous contributions from both the top and bottom surfaces of the overhang. Moreover, this may be an adequate assumption for a 2ft overhang, but the pressure on the bottom surface of a 4ft or 6ft or 12ft overhang is not a simple one-to-one wall-to-overhang pressure equivalent. The research that was done for canopies (ASCE 7-16 section 30.11), suggests that this is not the case (Zisis and Stathopoulos 2010, Candelario et al. 2014, Zisis et al. 2017). Most importantly the research that led to the revised provisions of ASCE 7-16 did not consider any building model with roof overhangs.

In this research project large scale wind tunnel testing will be carried out to clarify how the pressures on the wall relate to the overhang and for what distance, and at what point does the wall pressure cease to affect the overhang and the more direct wind loads on the overhang control, as though for an open building.

This interim report is mostly focusing on the previous research done on this topic and identifies their limitations and research gaps. It also includes the preliminary plan of the physical testing; i.e. model design, test setup and test protocols.

## **2. Previous studies on the effect of wind loads on roof overhangs**

The studies selected to be discussed in this section include both physical testing and numerical simulations. The findings provided information on the wind-induced loading on the upper and lower surface for the roof overhangs while considering different aspects and parameters (see Table

1). In an effort to better understand their contributions and limitations, the discussion is organized based on:

- The effect of roof geometry;
- The effect of overhang length;
- The interference effect of surrounding buildings on a single building with overhangs;
- Severe wind events and performance of roof overhangs;
- The effect of boundary wall locations on building with overhangs;
- Numerical simulation efforts to estimate wind loads on overhangs.

### ***2.1. Wind induced forces on eaves of low buildings with higher slope roof***

The effect of wind on eaves with higher slope roof (i.e. higher than  $10^\circ$ ) was studied by (Stathopoulos and Luchian 1994). The experiments of this study were conducted in the boundary layer wind tunnel of the Building Aerodynamics Laboratory at Concordia University. Two models were tested with a geometric scale of 1:400. Open county exposure was considered for all tests with a velocity profile represented by a power law with exponent of 0.15. The maximum wind speed at the gradient height in the tunnel was 13m/s. Two gable roof models with roof slopes of 4:12 and 12:12 were used for the measurements of the wind induced pressures on eaves. Each building was 40m wide and 60m long (at full scale), one with eave height of 5m and the other of 10m. The two models were equipped with pressure taps on lower and upper surfaces of the eave, as well as corresponding walls for comparison purposes.

This study found that the model with roof slope of 4:12 resulted into higher loads especially on the upper overhang surface and near the gable end. Positive pressures were found to be higher on the upper surface of roof with slope of 12:12, as expected from the wind flow considerations. Furthermore, it was found that the lower surface of the 4:12 slope was subjected to higher pressures and suctions. The eave height also had an effect on the pressure coefficients while the pressure measured on the wall surface and the eave lower surface compared well. However, some positive peaks under the eaves were significantly higher compared to the wall pressures.

### ***2.2. The assessment of wind loads on roof overhang with different lengths***

This study concluded that larger overhangs will influence the  $C_p$  values on both roofs and walls compared to roofs without overhangs or roofs with smaller overhangs. Wiik and Hansen (1997) investigated the effect of two overhangs of 0.3m and 3.4m on the wind load on the house walls. The study utilized both an experimental approach and numerical simulations. The experiments were conducted in the industrial aerodynamic wind tunnel of the University of Hertfordshire, UK while a commercial CFD code was used in the numerical simulations with a  $k-\epsilon$  turbulence model. Figure 1 shows a sketch for the house models with and without roof overhang at the gable wall.

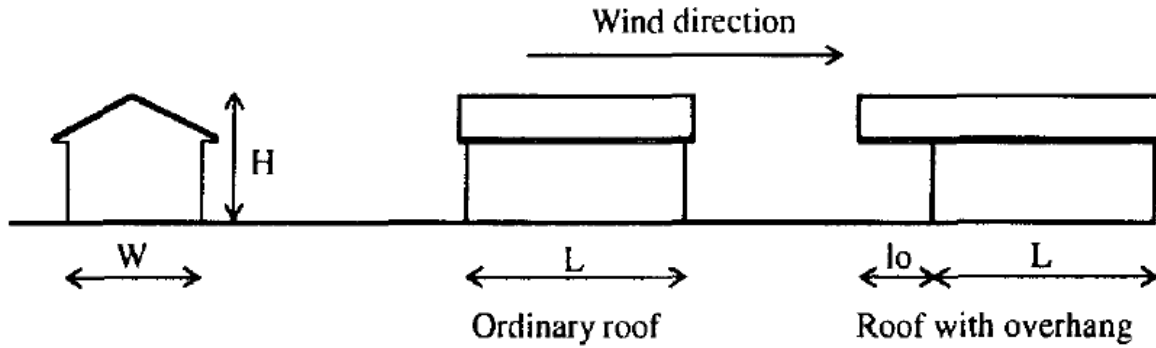


*Figure 1 Sketch shows the side view and elevation for the building model*

For the gable wall, in the case of the ordinary roof, the stagnation point occurred at  $2/3$  of the model height and then the pressure reduced towards the roof. For the large roof overhang model the stagnation point occurred at the top of the wall indicating that the upper part of the wall was subjected to higher wind forces compared to the ordinary roof. Moreover, the ordinary roof appeared to have higher  $C_p$  values near the edge compared to the large overhang roof. This was attributed to the high velocity in the  $z$ -direction at the edge of the ordinary roof, due to the nearby walls that lead part of the flow over the roof. Finally, it was concluded that large overhang will experience higher total uplift force due to the combination of pressure on the lower side and suction on the upper side.

### ***2.3. Field monitoring under extreme events and wind tunnel study of wind effects on roof overhangs***

The effect of roughness surface and turbulence intensity have a recognized effect on the induced pressure coefficients on both roofs and roof overhangs. Wang et al. (2020) presented results from a field study during Typhoons Mujigae and Sarika, which was also supported by detailed wind tunnel tests on a 1:50 scaled model of the low-rise gable roof building that was used during the field measurements. Three terrain exposures were generated in the wind tunnel corresponding to three surface roughness length,  $z_0=0.3\text{m}$ ,  $z_0=0.087\text{m}$ , and  $z_0=0.03\text{m}$ . The model was instrumented with pressure taps on the upper and lower surface of the roof overhang in both model and full-scale measurements. Pressure coefficients on the upper and lower surfaces, and net pressure coefficients of the roof overhang were discussed in detail in this study.

It was found that as the turbulence intensity increases, the maximum magnitude of the RMS and minimum pressure coefficients increases. The correlation coefficients of wind pressure were significantly influenced by the turbulence intensity on the front edge of the overhang and edge near the building wall, while the turbulence intensity had a little effect on the correlation coefficients on the corner of the roof overhang.

The variation of the different pressure coefficients (mean, RMS, max and min) shows a good agreement between the wind tunnel measurements and the field measurements. However, the reduced scale experimental results underestimated the peak coefficients compared to field measurements, which was attributed to the Reynolds number mismatch between the wind tunnel

and the full-scale tests. Finally, the comparison of the experimental results - model scale and full-scale – to the ASCE 7-16, showed that ASCE 7 was in general more conservative.

#### ***2.4. Numerical simulations to study the wind loads on overhangs***

(Majid et al. 2016) investigated the effect of roof overhang length on the pressure coefficient underneath the overhang considering also the presence of an attached secondary space directly below the overhang. The CFD analysis used the Reynolds-averaged Navier-Stokes equations (RANS) with an RNG k- $\epsilon$  turbulence model. Four lengths were used, including 0.5m, 0.75m, 1.0m, and 1.25m overhangs while the roof for the four models had the same pitch of 27°. The study showed that the diameter of the recirculation eddy increased with increasing the overhang length. The highest positive pressure coefficient was formed at the wall underneath the 0.5m overhang, due to the smaller eddies that were formed and lead the flow to impinge the wall directly.

#### ***2.5. Effect of overhangs on wind pressures on low-rise hip roof buildings***

In this study (Ahmad and Kumar 2002) studied the effect of different overhang length and eave height aspect ratios on the wind pressures on a hip roof with pitch of 30°. The focus of this study was on the main roof loads rather than the overhang areas. Experiments were carried out in a wind tunnel at the University of Roorkee, Roorkee (India). Six hip roof building models of a building 14m x 7m and 2.9m eave height were constructed at 1:50 scale. Three of models had overhang lengths of 0.5m, 0.75m and 1.1m while the height remained constant and the aspect ratio was 0.4. The remaining three models has variable height and aspect ratios of 0.4, 0.5 and 0.6 while the overhang length was fixed at 1.1m.

Both the overhang and aspect ratio variations were found to influence the magnitude and distribution of pressures on the hip roof. The maximum peak pressures among the three overhangs have been found to occur at the edge corner of the 0.75m overhang. The peak pressure on the corner edge for the 1.1m overhang was also high but a bit smaller than the peak pressure of the 0.75m overhang.

#### ***2.6. Experimental study of wind loads on gable roofs of low-rise buildings with overhangs***

The wind pressure distribution on gable roofs with overhangs was investigated by Huang et al. (2018) through an extensive amount of wind tunnel tests. The study considered 99 test cases with various roof pitches, height-depth ratios and width-depth ratios. The experiments were conducted at Tongji University and the models included cases with 11 different roof pitches, 3 different height-depth ratios, and 3 different width-depth ratios. Pressure taps were placed on the upper and lower surfaces of the roof overhangs.

For roof pitch of 0° to 9.5°, the negative block (i.e. area averaged) pressure coefficient increased while for roof pitch larger than 9.5°, the block pressure coefficient linearly decreased. The negative block pressure coefficients on overhangs decreased from – 2.0 at the roof pitch of 0°– 10° to a positive block pressure coefficient of 0.1 at the roof pitch of 60°.

## 2.7. Wind load on overhangs in a low gable building in presence of free-standing wall

Some studies investigated the presence of a free-standing wall or the interference of other buildings on loads on overhangs. John et al. (2008) experimentally studied the effect of a free-standing wall (boundary wall) on the pressure variation on the overhang for a gable roof building with a 25° slope. The wind tunnel model was at 1:25 scale and the overhang length was 1.5m at full scale. The study found that the edge of the overhang experiences severe changes in pressure values with change in the distance of the boundary wall from the parent building. It was found that the maximum value of the net positive pressure was when the free-standing wall was located at a distance 3h from the building, where h is the building height. For a stand-alone case without the wall, the overhang experienced the maximum negative net pressure. On a follow up study, John et al. (2011) examined the interference effect of boundary wall on pressure variation on the roof overhang, the roof, and the wall for a gable roof building. Overall, it was concluded that the boundary walls may significantly reduce the wind pressures on roof overhangs while this interference effect reaches its maximum up to a certain distance after which there is practically no effect.

**Table 1 Summary of parameters and findings in previous studies**

<i>Different Aspects</i>	<i>Methodology</i>	<i>Findings</i>	<i>Notes</i>
<i>Roof Geometry (Stathopoulos and Luchian 1994)</i>	<i>- Two gable roof models with slopes 4:12 and 12:12 were studied</i>	<ul style="list-style-type: none"> <li>- Positive pressure on the upper surface found to be higher on the 12:12 slope.</li> <li>- Higher pressure and suction at 4:12 slope</li> </ul>	
<i>Roof Geometry (Huang et al. 2018)</i>	<i>- 99 models all with overhangs have 11 different roof pitches, 3 different height-depth ratios, and 3 different width-depth ratios.</i>	<i>- Negative block pressure coefficients on overhang decreased from – 2.0 at the roof pitch of 0°– 10° to a positive block pressure coefficient of 0.1 at the roof pitch of 60°.</i>	
<i>Length of Overhang (Wiik and Hansen 1997)</i>	<i>- Cp values on two models with two overhangs length 0.3m, 3.4m were studied experimentally.</i>	<ul style="list-style-type: none"> <li>- Different location for stagnation point between the two models.</li> <li>- Higher wind force in case of the large overhang.</li> <li>- Higher Cp near the upper edge for shorter overhang.</li> <li>- Higher up lift force in the larger overhang</li> </ul>	
<i>Length of Overhang (Majid et al. 2016)</i>	<i>- A numerical investigation studied the effect of four overhangs (0.5m, 0.75m, 1.0m and 1.25m) on Cp underneath the overhang.</i>	<ul style="list-style-type: none"> <li>- Diameter of the recirculation eddy increased with increasing the overhang length.</li> <li>- Highest wall pressure occurred underneath the shortest overhang.</li> </ul>	

<i>Length of Overhang (Ahmad and Kumar 2002)</i>	<i>- In other experimental study hip roof models with overhang length (0.5m, 0.75m and 1.0m) were studied for Cp coefficients.</i>	<i>- Overhangs were found to influence magnitude and distribution of pressure on roof. - Max peak pressure were found at the edge corner of 0.75m overhang.</i>	
<i>Interference of walls (John et al. 2008)</i>	<i>- Cp coefficients on overhang in a gable roof building with the presence of a boundary wall located around the building.</i>	<i>- The maximum value of the net positive pressure was at a case when the free-standing wall located a distance 3h from the building, where h is the building height. - The overhang experienced the maximum negative net pressure when there was no wall.</i>	
<i>Effect of Roughness surface (Wang et al. 2020)</i>	<i>- A model was tested for three roughness surfaces, zo= (0.3m, 0.087m and 0.03m)</i>	<i>- Increasing the turbulence intensity, causes increase in the magnitude of minimum pressure on overhangs.</i>	<i>- This study included a codification with ASCE 7-16 and Chinese design code</i>

### 3. Limitations of previous studies and recommendations

The previous studies on roof overhangs included different configurations and valuable findings related to pressure coefficients on overhangs. However, some of these studies had some limitations that need to be considered and help us identify research gaps and priorities. For instance, Wiik and Hansen (1997) examined two models with two rather extreme lengths for roof overhangs (i.e. 0.3m and 3.4m) and did not consider intermediate lengths. Ahmad and Kumar (2002) examined three lengths of roof overhangs (i.e. 0.5m, 0.75m and 1.0m) and it was found that the 0.75m overhang had the maximum negative peak Cp while the 1.0m overhang had the lowest value. Lengths over 1m might provide additional details on the behavior of longer overhangs. Majid et al. (2016) examined four lengths of roof overhangs numerically which is not expected to provide valuable input from a codification point of view.

In summary, previous studies did not adequately examine the relation between the Cp magnitude at adjacent walls and underneath the roof overhang. Moreover, there was not enough knowledge at what length of the overhang does the Cp differ from the adjacent wall Cp (i.e. basic assumption implemented by ASCE7-16). Finally, smaller-scale models did not allow for high pressure tap resolution and did not consider any Reynolds number effects.

Therefore, in the current preliminary study, it is proposed to perform physical testing at a large scale and consider the following configurations:

- Configuration 1: A Hip roof of slope 4:12 with a short overhang to study the variation of Cp on the upper and lower surface of the overhang, and on the adjacent wall, and determine

the different locations of stagnation point for each case. This shall be used for codification purposes with ASCE 7-16.

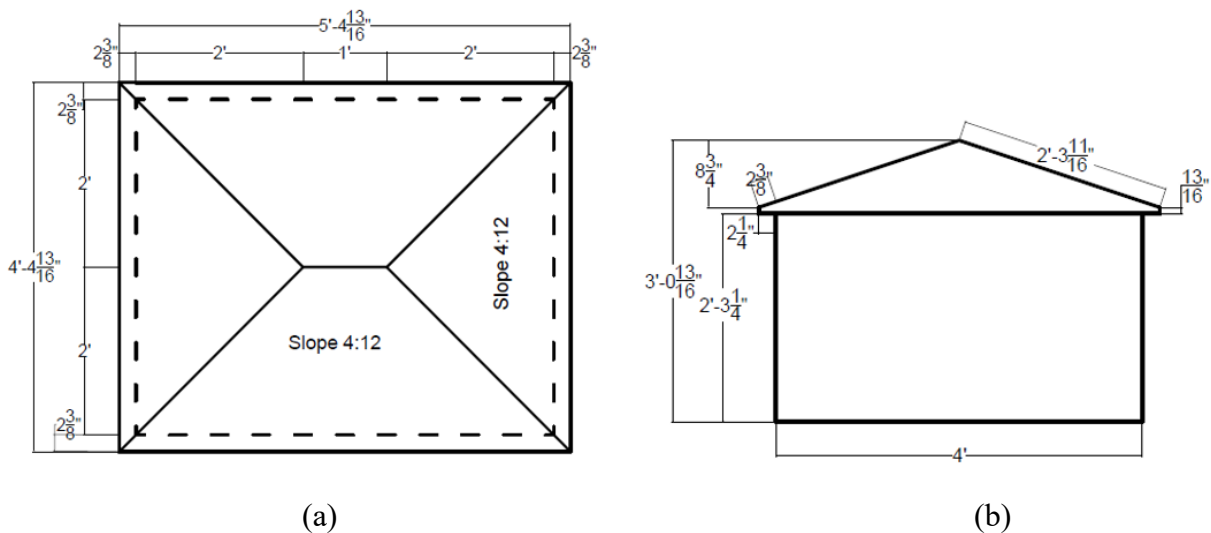
- Configuration 2: A Hip roof with slope 4:12 with a long overhang (e.g. 6 ft in length) to study the effect of longer overhangs on the variation of pressure coefficient on adjacent wall and compare it to Case 1.

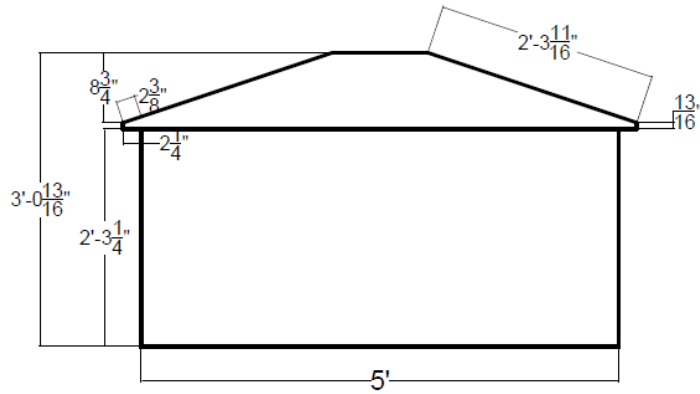
#### 4. Proposed experimental setup

This section comprises the proposed experimental test setup that will be conducted at the Wall of Wind (WOW) Experimental Facility at Florida International University (FIU) (Gan Chowdhury et al. 2016). The 12-fan WOW is the largest and most powerful university research facility of its kind and is capable of simulating a Category 5 hurricane – the highest rating on the Saffir-Simpson Hurricane Wind Scale. In 2015, the National Science Foundation (NSF) has designated the Wall of Wind as one of the nation’s major “Experimental Facilities” (EF) under the Natural Hazards Engineering Research Infrastructure (NHERI) program as a distributed, multi-user national facility that provides the natural hazards research community with access to research infrastructure. The WOW EF is managed by FIU’s Extreme Events Institute (EEI).

##### 4.1. Model layouts and dimensions

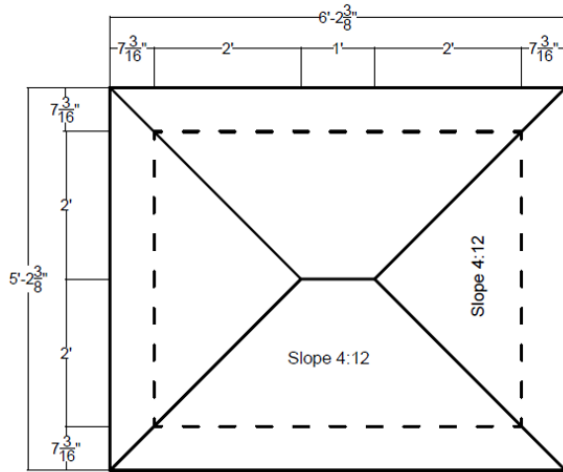
Following discussions with an informal advisory group of building code officials and truss manufacturing companies, it was concluded that priority should be given to the most common layouts that exist in current residential construction market. Thus, a hip roof building layout was selected, with slope 4:12, eave height of 24ft and horizontal dimensions of 40ft by 50ft (full scale). To take full advantage of WOW’s large experimental section, a geometric scale of 1:10 will be used. The first model (Configuration A) will have an inclined overhang length of 2ft which is one of the most common length suggested by the truss manufacturing industry, while the other model (Configuration B) will use an inclined overhang length of 6ft which is also relatively common in the State of Florida. Preliminary drawings of the two configurations are shown in Figure 2 and Figure 3 respectively.



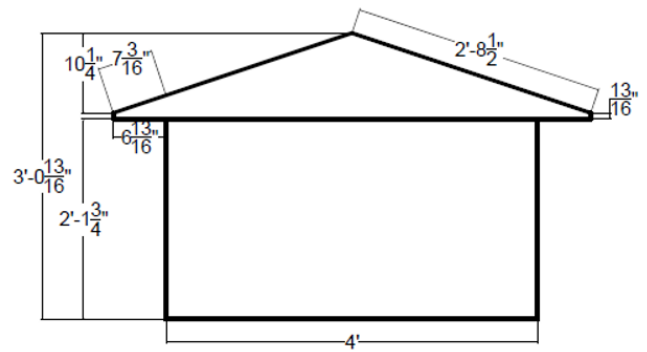


(c)

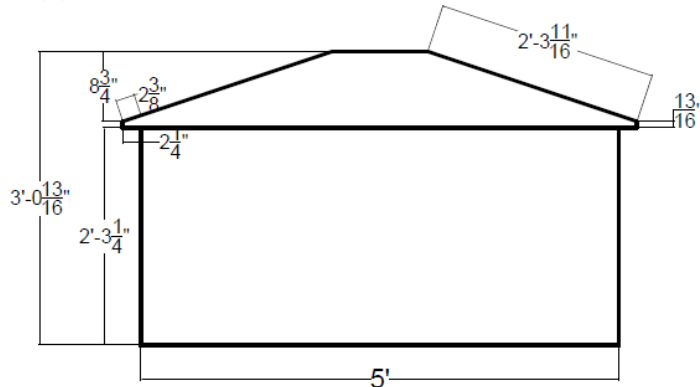
**Figure 2 Configuration A model layout (a) Plan View (b) Side View (c) Elevation View**



(a)



(b)



(c)

**Figure 3 Configuration B model layout (a) Plan View (b) Side View (c) Elevation View (all dimensions are at model-scale)**

Table 2 shows the scales for the different parameters in test setup and Table 3 shows the prototype and model dimensions. Froude number and Strouhal number were preserved and kept constant between the full scale (prototype) and the scaled model. Froude number is a dimensionless number defined as the ratio between the inertial force to the external field ( $F = \frac{V}{\sqrt{gL}}$ , where V is the flow velocity, g is the gravitational acceleration, L is the characteristic length). Since the gravitational acceleration is the same between the prototype and the model, the velocity scale is related to the square root of the length scale. Strouhal number is a dimensionless number describing the flow mechanism oscillation ( $S = \frac{FL}{V}$  where F is the vortex shedding frequency, L is the characteristic length and V is the flow velocity). Thus, the frequency scale has been related to the velocity and length scale accordingly. The time scale was calculated as the reciprocal of the frequency scale which is the same as the ratio between the length scale to the velocity scale.

**Table 2 Testing parameters scale factors**

<i>Parameters</i>	<i>Scale Factor</i>
<i>Length</i>	<i>1:10</i>
<i>Velocity</i>	<i>1:<math>\sqrt{10}</math></i>
<i>Frequency</i>	<i><math>\sqrt{10}</math></i>
<i>Time</i>	<i>1:<math>\sqrt{10}</math></i>

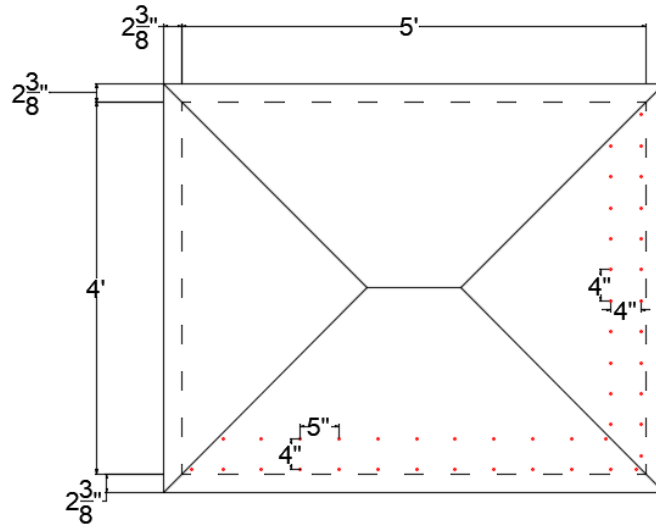
**Table 3 Prototype and scaled model dimensions**

<i>Configuration</i>	<i>Model</i>	<i>Roof Slope</i>	<i>Building Dimensions</i>		<i>Scale</i>	<i>Model Dimensions</i>	
			<i>L x W x h</i> <i>(ft)</i>	<i>Overhang</i> <i>(ft)</i>		<i>L x W x h</i> <i>(ft)</i>	<i>Inclined Overhang</i> <i>(in)</i>
<i>A</i>	<i>Hip Roof</i>	<i>4:12 (18.4°)</i>	<i>50 x 40 x 24</i>	<i>2</i>	<i>1:10</i>	<i>5 x 4 x 2.4</i>	<i>2.4</i>
<i>B</i>	<i>Hip Roof</i>	<i>4:12 (18.4°)</i>	<i>50 x 40 x 24</i>	<i>6</i>	<i>1:10</i>	<i>5 x 4 x 2.4</i>	<i>7.2</i>

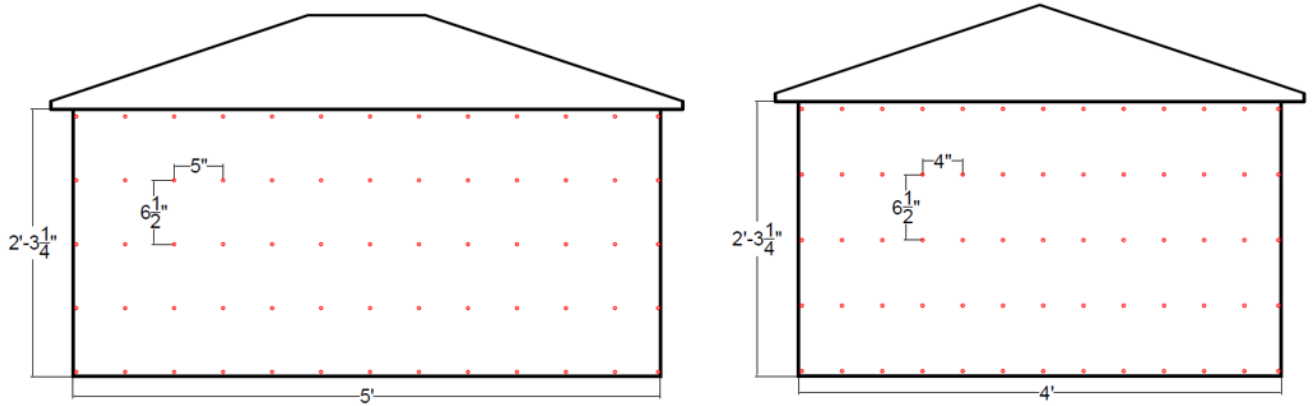
#### **4.2. Instrumentation and test protocol**

Pressure taps will be added on the walls, the top surface of overhangs and the bottom surface of soffits, as well as on the roof area adjacent to overhangs to be placed within zone 3 and 2e as specified in ASCE 7-16. The pressure taps will be connected to a sensitive pressure scanning system (Scanivalve ZOC33). The maximum pressure that could be measured by this module is 0.36 psi (51.84 psf). This pressure could be reached at about 90 mph for smooth flow, and about 60 mph for turbulent flow.

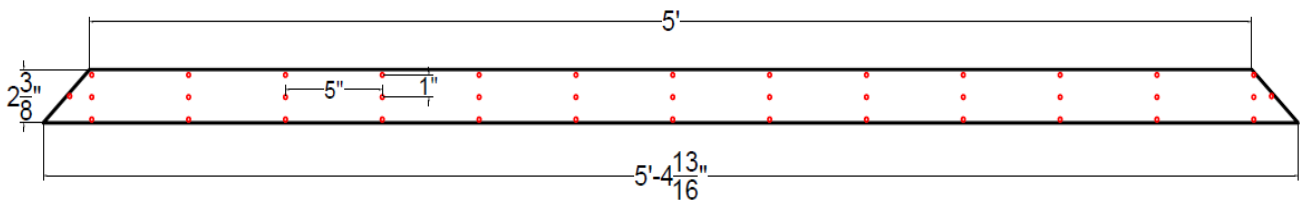
Configuration A will have 340 pressure taps and Configuration B will have 374 pressure taps (i.e. wall, overhang, and roof surface). Pressure tap locations are shown in Figure 4 and Figure 5. The test will be conducted for 40 wind direction for each model (i.e.  $0^\circ \rightarrow 360^\circ$  with increments of 10 degrees plus the four corners) with a target wind speed of 60 mph. The sampling time for each direction is 60 seconds and the sampling frequency is 520 (Hz). The two models will be tested for an open terrain exposure (i.e. category ‘C’).



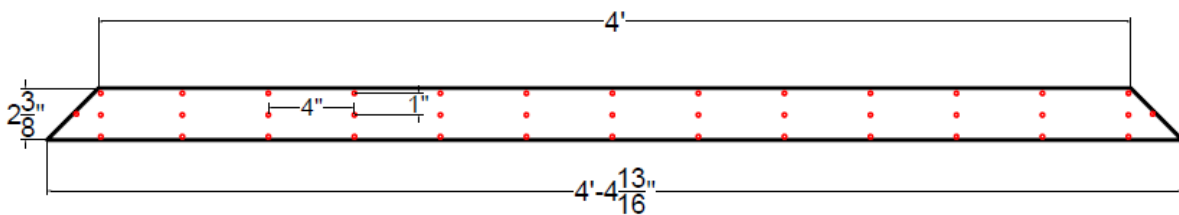
(a)



(b)

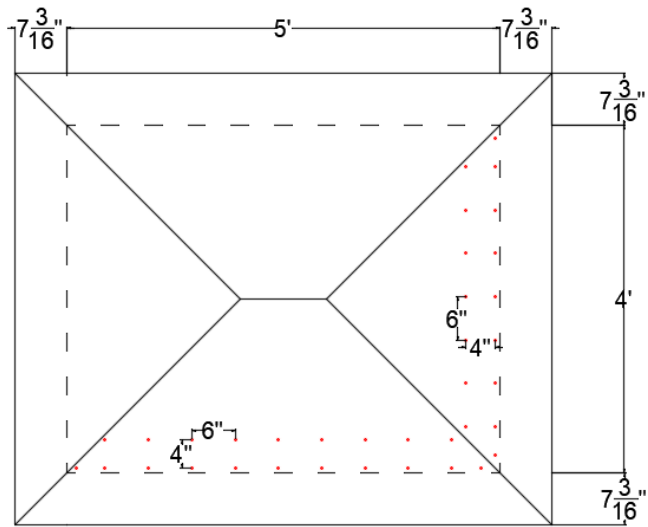


(c)

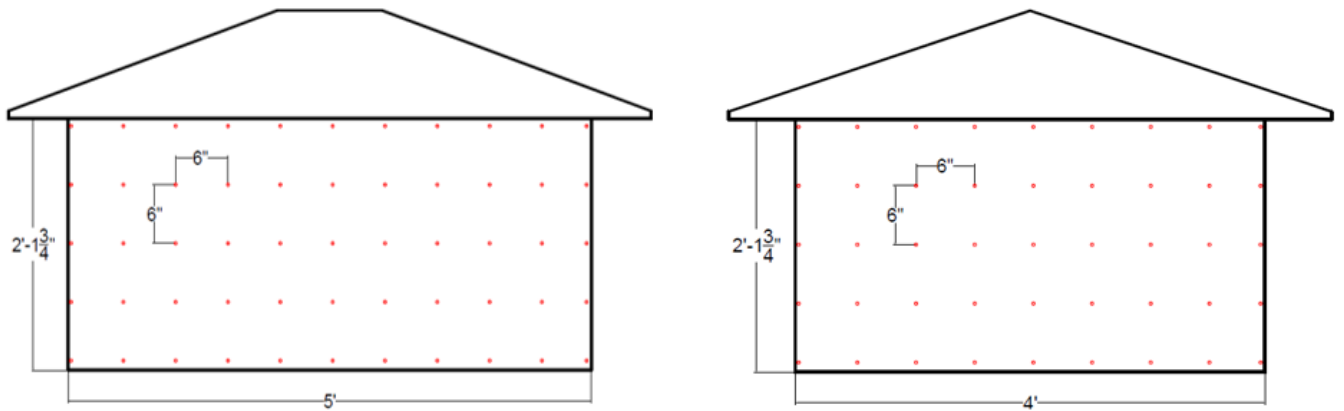


(d)

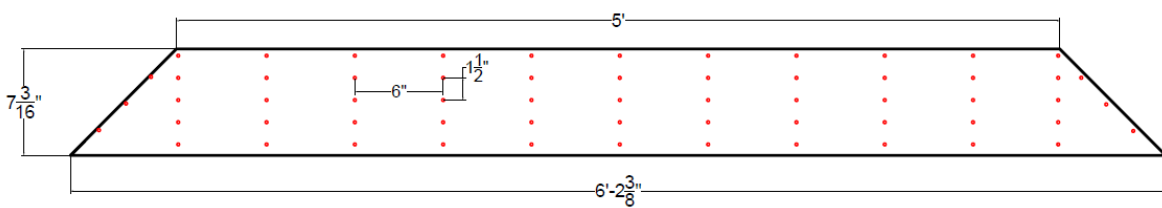
**Figure 4 Pressure taps instrumentation on configuration A model (a) Roof (b) Longitudinal and Side Walls (c) Longitudinal overhang (d) Side overhang.**



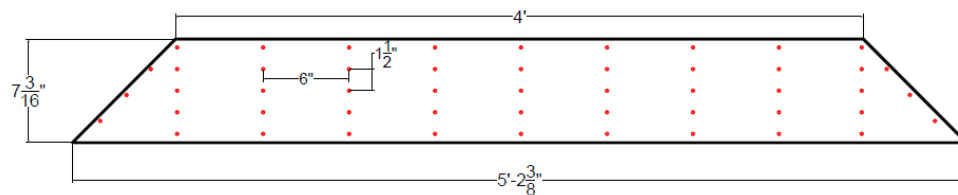
(a)



(b)



(c)



(d)

**Figure 5 Pressure taps instrumentation on configuration B model (a) Roof (b) Longitudinal and Side Walls (c) Longitudinal overhang (d) Side overhang.**

## References

- Ahmad, S., and Kumar, K. (2002). "Effect of geometry on wind pressures on low-rise hip roof buildings." *Journal of Wind Engineering and Industrial Aerodynamics*. Vol. 90 (7), 755-779.
- ASCE. (2010). "*Minimum design loads for building and other structures.*" American Society of Civil Engineers, ASCE/SEI 7-10, Reston, VA.
- ASCE. (2017). "*Minimum Design Loads and Associated Criteria for Buildings and Other Structures.*" American Society of Civil Engineers, ASCE/SEI 7-16, Reston, VA.
- Candelario, J. D., Stathopoulos, T., and Zisis, I. (2014). "*Wind Loading on Attached Canopies: Codification Study.*" *Journal of Structural Engineering*, 140(5), 04014007.
- Gan Chowdhury, A., Zisis, I., Irwin, P., Bitsuamlak, G., Pinelli, J.-P., Hajra, B., and Moravej, M. (2017). "Large-Scale Experimentation Using the 12-Fan Wall of Wind to Assess and Mitigate Hurricane Wind and Rain Impacts on Buildings and Infrastructure Systems." *Journal of Structural Engineering*, Vol. 143, Issue 7.
- Huang, P., Tao, L., Gu, M., and Quan, Y. (2018). "Experimental study of wind loads on gable roofs of low-rise buildings with overhangs." *Frontiers of Structural and Civil Engineering*, 12(3), 300–317.
- John, A. D., Gairola, A., and Krishna, P. (2008). "Wind Loads on Overhangs in a Low Gable Building in Presence of Free Standing Wall." *Journal of Wind and Engineering*, 5(1), 39–46.
- John, A. D., Singla, G., Shukla, S., and Dua, R. (2011). "Interference effect on wind loads on gable roof building." *Procedia Engineering*, Elsevier B.V., 14, 1776–1783.
- Majid, T. A., Zaini, S. S., Ismail, M. A., Deraman, N. C., and Poon, J. L. (2016). "Numerical investigation on the effect of overhang roof around rural house." *The 2016 World Congress on Advances in Civil, Environmental, and Materials Research (ACEM16)*.
- Stathopoulos, T., and Luchian, H. (1994). "Wind-induced forces on eaves of low buildings." *Journal of Wind Engineering and Industrial Aerodynamics*, 52(C), 249–261.
- Taher, R. (2007). "Design of Low-Rise Buildings for Extreme Wind Events." *Journal of Architectural Engineering*, 13(1), 54–62.
- Wang, X., Li, Q., and Li, J. (2020). "Field monitoring and wind tunnel study of wind effects on roof overhang of a low-rise building." *Structural Control and Health Monitoring*, 27(3), 1–25.
- Wiik, T., and Hansen, E. W. M. (1997). "The assessment of wind loads on roof overhang of low-rise buildings." *Journal of Wind Engineering and Industrial Aerodynamics*, 67–68, 687–696.

Zisis, I., and Stathopoulos, T. (2010). "Wind-Induced Pressures on Patio Covers." *Journal of Structural Engineering*, 136(9), 1172–1181.

Zisis, I., Raji, F. and Candelario, J. D. (2017). "Large scale wind tunnel tests of canopies attached to low-rise buildings." *ASCE Journal of Architectural Engineering*, Vol. 23 (1).